New Computational Challenges in Fluid–Structure Interactions Problems

S.R. Idelsohn*, E. Oñate, R. Rossi, J. Marti, and F. Del Pin

Abstract In this paper the so-called added-mass effect is investigated from a different point of view of previous publications. The monolithic fluid structure problem is partitioned using a static condensation of the velocity terms. Following this procedure the classical stabilized projection method for incompressible fluid flows is introduced. The procedure allows obtaining a new pressure segregated scheme for fluid-structure interaction problems which has good convergent characteristics even for biomechanical application, where the added mass effect is strong. The procedure reveals its power when it is shown that the same projection technique must be implemented in staggered FSI methods.

Keywords Fluid-structure interactions · Added mass effect · Incompressible flows · Pressure segregation

1 Introduction

Fluid-structure interaction problems involving an incompressible viscous flow and elastic non-linear structure have been solved in the past using different methods: *Partitioned (or staggered)* [1–4] approaches are probably the most popular solution technique for the simulation of coupled problems as they allow using specifically designed codes on the different domains and offer significant benefits in terms of

S.R. Idelsohn, E. Oñate, R. Rossi, and J. Marti
International Center for Numerical Methods in Engineering (CIMNE), Universitat Politécnica de Catalunya (UPC), Gran Capitan s/n, Barcelona, Spain
*ICREA Research Professor at CIMNE

F. Del Pin
Livermore Software Technology Corporation, 7374 Las Positas Road, Livermore 94551, CA, USA

J. Eberhardsteiner et al. (eds.), *ECCOMAS Multidisciplinary Jubilee Symposium*, Computational Methods in Applied Sciences.

efficiency: smaller and better conditioned subsystems are solved instead of a single problem. *Loosely (or weakly)* [5] and *strongly coupled* [6–12] schemes are distinguished in the partitioned case: loosely coupling schemes require only one solution of either field per time step in a sequentially staggered manner and are thus particularly appealing in terms of efficiency. Strongly coupled schemes give, after an iterative process, the same results as non-partitioned (also named *monolithic*) algorithms. Both of them, the strongly coupled as well as the monolithic scheme, lead to expensive simulations since, at each time step, a sub iteration algorithm including the fluid and the structure domain have to be performed in the partitioned strongly coupled scheme. Alternatively, fully coupled systems including the equations for the fluid and structure must be solved for the monolithic procedure.

There is a key difference between the strongly coupled scheme and the monolithic scheme: the iterative process in the strongly coupled scheme may be difficult (even non-convergent) when the so-called "*added-mass effect*" is important [13, 14]. Indeed, in such situation, a monolithic scheme seems to be necessary to avoid numerical instabilities. The name "*added-mass effect*" has been used in the literature to indicate the instabilities that typically occur in the internal flow of an incompressible fluid whose density is close to the structure density. We will use the same terminology to be consistent with previous papers, but as will be shown later, the instabilities are not necessarily caused by a fluid density close to the structure density. There are other factors, as elasticity coefficients and time step size that must be taken into account to avoid unstable solutions. The added-mass effect is not present in aero elasticity problems, but it becomes very important in biomechanics applications where the materials are normally muscles and arteries and the fluid is blood.

Weakly coupled schemes are also affected by the added-mass effect: they become unstable when this effect is significant.

There is a third situation for which the added-mass effect produces complications. It concerns the monolithic solution of the fluid-structure interaction problem when the pressure is segregated from the displacement or the velocity fields. In this case, even if we are solving together in a coupled way the fluid and the solid equations, the iterative scheme to obtain the pressure may be difficult and even non-convergent.

The purpose of this paper is to put in evidence that the added-mass effect is a consequence of the pressure segregation (case 3 in the previous list) and that a correct understanding of the pressure segregation effect yields different solutions to the added-mass problem which may be successfully applied to cases 1 and 2.

The segregation of the pressure can be conveniently performed using a Chorin-Temam projection scheme [15, 16]. This splitting procedure works conveniently for incompressible flows. Nevertheless we will introduce pressure segregation via a simple static condensation procedure. This static condensation will explain the Chorin Teman projection as a particular case and will allow generalizing the Chorin-Temam scheme for fluid–structure interaction problems.

2 The Discretized Equations to Be Solved in a FSI Problem

The equations to be solved for both the incompressible fluid and the elastic solid domains are the momentum equations:

$$\rho a_i = \rho \frac{DV_i}{Dt} = \frac{\partial \sigma_{ij}}{\partial x_j} + \rho f_i \tag{1}$$

where σ_{ij} is the Cauchy stress tensor, ρ the density, a_i the acceleration vector equal to the total derivative of the velocity V_i and f_i a body force vector.

In the incompressible part of the domain, mass conservation must be enforced:

$$\varepsilon_V = \frac{\partial V_i}{\partial x_i} = 0, \tag{2}$$

and the boundary conditions for both domains are:

$$\sigma_{ni} = \bar{\sigma}_{ni} \text{ in } \Gamma_\sigma \text{ and } U_i = \overline{U_i} \text{ in } \Gamma_U \tag{3}$$

On the fluid domain, it is sometimes useful to use a moving framework different than the particle displacement. In this case, the acceleration vector may be written as a function of the framework velocity V_{Mj} as:

$$\frac{DV_i}{Dt} = \frac{D_F V_i}{Dt} + (V_j - V_{Mj}) \frac{\partial V_i}{\partial x_j} \tag{4}$$

where $\frac{D_F V_i}{Dt}$ represents the framework derivative of the velocity.

Apart from the incompressible condition the only difference between the fluid and the solid are the constitutive equations. Nevertheless, once the time integration scheme has been chosen, both constitutive equations may be written as a function of the displacement rates or the velocities rates (adding always the pressure in the incompressible part).

Assuming for simplicity that an implicit Euler time integration has been chosen, then:

$$U_i^{n+1} = \Delta t \left(\theta V_i^{n+1} + (1-\theta) V_i^n \right) \tag{5}$$

where the upper index indicates the time position, Δt is the time step and θ is an integration parameter between 0 and 1. To simplify the notation, in the following the upper index $n+1$ will be omitted.

In the following and without lack of generality, we will consider that the constitutive equations for the solid and the fluid domains are expressed as a function of the velocity field (plus the pressure in the incompressible regions). The same results and conclusions may be obtained using the displacements as the main unknowns.

The weighted residual form of the momentum and mass conservations equations are:

$$\int_V W_l \left(\rho \frac{DV_i}{Dt} - \frac{\partial \sigma_{ij}}{\partial x_j} - \rho f_i \right) dV + \int_{\Gamma_\sigma} W_l (\sigma_{ni} - \overline{\sigma_{ni}}) d\Gamma = 0 \tag{6}$$

$$\int_V W_p (-\varepsilon_V) dV = 0 \tag{7}$$

and the weak form is:

$$\begin{aligned} &\int_V \left[W_l \left(\rho \frac{DV_i}{Dt} \right) + \frac{\partial W_l}{\partial x_j} \sigma_{ij} - W_l \rho f_i \right] dV - \int_{\Gamma_\sigma} W_l \overline{\sigma_{ni}} d\Gamma = 0 \\ &\int_V W_p (-\varepsilon_V) dV = 0 \end{aligned} \tag{8}$$

Replacing the stress tensor from the corresponding constitutive equation and discretizing the velocity and the pressure fields with standard shape functions:

$$V_i = \mathbf{N}^T \mathbf{V}_i \tag{9}$$

$$p = \mathbf{N}_p^T \mathbf{P} \tag{10}$$

and using Galerkin weighting functions the global fluid–structure interaction problem may be written in a compact monolithic form as:

$$\begin{bmatrix} \left(\frac{\mathbf{M}_\rho}{\Delta t} + \mathbf{K} \right) & -\mathbf{B} \\ -\mathbf{B}^T & 0 \end{bmatrix} \begin{bmatrix} \mathbf{V} \\ \mathbf{P} \end{bmatrix} = \begin{bmatrix} \mathbf{F} + \frac{\mathbf{M}_\rho}{\Delta t} \mathbf{V}^n \\ 0 \end{bmatrix} \tag{11}$$

where $\mathbf{M}_\rho$ is the mass matrix which is a function of the fluid density ρ_f or the solid density ρ_s and the shape functions: with $\mathbf{K}_{ij} = \mathbf{K}_{ij}^1 + \mathbf{K}_{ij}^2 + \mathbf{K}_{ij}^3$. In the fluid part:

$$\mathbf{K}_{ii}^1 = \int_V \frac{\partial \mathbf{N}}{\partial x_j} \mu \frac{\partial \mathbf{N}^T}{\partial x_j} dV; \tag{12a}$$

$$\mathbf{K}_{ij}^2 = \int_V \frac{\partial \mathbf{N}}{\partial x_j} \mu \frac{\partial \mathbf{N}^T}{\partial x_i} dV; \tag{12b}$$

$$\mathbf{K}_{ij}^3 = \int_V \frac{\partial \mathbf{N}}{\partial x_i} \left(-\frac{2\mu}{3} \right) \frac{\partial \mathbf{N}^T}{\partial x_j} dV, \tag{12c}$$

and in the solid domain:

$$\mathbf{K}_{ii}^1 = \int_V \frac{\partial \mathbf{N}}{\partial x_j} \left(\frac{\Delta t G}{J} \right) \frac{\partial \mathbf{N}^T}{\partial x_j} dV; \tag{13a}$$

$$\mathbf{K}_{ij}^2 = \int_V \frac{\partial \mathbf{N}}{\partial x_j}\left(\frac{\Delta t G}{J}\right)\frac{\partial \mathbf{N}^T}{\partial x_i}dV; \tag{13b}$$

$$\mathbf{K}_{ij}^3 = \int_V \frac{\partial \mathbf{N}}{\partial x_i}\left(\frac{\Delta t \lambda}{J}\right)\frac{\partial \mathbf{N}^T}{\partial x_j}dV \tag{13c}$$

In the case where the moving framework is different than the particle displacement matrix $\mathbf{K}$ includes the convective terms $\mathbf{K}_{ij}^4$:

$$\mathbf{K}_{ii}^4 = \int_V \mathbf{N}(V_j - V_{Mj})\frac{\partial \mathbf{N}^T}{\partial x_j}dV \tag{14}$$

Matrix $\mathbf{B}$ affects the incompressible part of the domain. This means that $\mathbf{B}$ has non-zero terms only in the degrees of freedom related with the fluid including the interfaces solid–fluid.

The form of matrix $\mathbf{B}$ is:

$$\mathbf{B}^T = [\mathbf{B}_1^T, \mathbf{B}_2^T, \mathbf{B}_3^T] \text{ with } \mathbf{B}_i^T = \int_V \mathbf{N}_p \frac{\partial \mathbf{N}^T}{\partial x_i}dV \tag{15}$$

Equation (11) represent the coupled monolithic fluid–structure interaction problem that must be solved. It is well known that this system of equations must be stabilized for some class of equal order interpolations (e.g. when $\mathbf{N}_p = \mathbf{N}$) [17].

Independently of the method chosen to stabilize the problem, we will assume that the problem has been conveniently stabilized by a matrix $\mathbf{S}$ in such way that the problem reads:

$$\begin{bmatrix} \left(\frac{\mathbf{M}_\rho}{\Delta t} + \mathbf{K}\right) & -\mathbf{B} \\ -\mathbf{B}^T & \mathbf{S} \end{bmatrix} \begin{bmatrix} \mathbf{V} \\ \mathbf{P} \end{bmatrix} = \begin{bmatrix} \mathbf{F} + \frac{\mathbf{M}_\rho}{\Delta t}\mathbf{V}^n \\ 0 \end{bmatrix} \tag{16}$$

3 Monolithic Solution of the FSI Equations by Pressure Segregation

Solution of the Eq. (16) as a fully coupled system of equations is sometimes expensive due to ill-conditioning problems. A more convenient way to solve this system is segregating the pressure from the remaining unknowns (in our examples the velocity field). Segregation means to separate during the solution process the pressure from the velocity variables in a staggered way: first the velocities (or the pressure) are evaluated independently of the pressure (or the velocities) and then the solution of the pressure (or the velocities) is found using the previous results. Segregation of the pressure has several advantages as:

1. Decreases the number of degrees of freedom to be solved simultaneously
2. Avoid ill-conditioned matrices

3. Allows using unified formulations for fluid and solid
4. Allows us to draw some conclusions to be used in partitioned schemes (in which the pressure is always segregated from the solid part)

There are several ways to segregate the pressure from the velocity. The simplest one is to assume an initial value for the pressure, compute the velocities using this initial value and then evaluate the pressure iteratively. A more sophisticated scheme to segregate the pressure is the Chorin-Temam projection scheme [15, 16] which will be discussed later.

In order to easy the discussion the algorithm to be presented next, the following change of variable will be introduced: Being $\mathbf{P}_0$ anyarbitrary vector of the same dimension of the pressure, the following new unknown will be defined:

$$\delta\mathbf{P} = \mathbf{P} - \mathbf{P}_0 \tag{17}$$

Note that $\mathbf{P}_0$ is not necessarily the initial pressure vector at time $t = 0$.

The system of equations to be solved becomes:

$$\begin{bmatrix} \left(\frac{\mathbf{M}_\rho}{\Delta t} + \mathbf{K}\right) & -\mathbf{B} \\ -\mathbf{B}^T & \mathbf{S} \end{bmatrix} \begin{bmatrix} \mathbf{V} \\ \delta\mathbf{P} \end{bmatrix} = \begin{bmatrix} \mathbf{F} + \frac{\mathbf{M}_\rho}{\Delta t}\mathbf{V}^n \\ -\mathbf{S}\mathbf{P}_0 \end{bmatrix} \tag{18}$$

3.1 Static Condensation of the Pressure

The only way to segregate exactly the pressure from the velocity is via static condensation. Static condensation is a procedure to solve a system of equations in a partitioned way. It consists of inverting a part of the initial matrix. For instance in system (18) we can condensate the pressure by inverting matrix $\mathbf{S}$, or condensate the velocity by inverting matrix $\left(\frac{\mathbf{M}_\rho}{\Delta t} + \mathbf{K}\right)$. Matrix $\mathbf{S}$ must be singular and then the only possibility is to statically condense the velocity field.

From the first row of (18) the velocity field may be obtained as:

$$\mathbf{V} = \left(\frac{\mathbf{M}_\rho}{\Delta t} + \mathbf{K}\right)^{-1} \left(\mathbf{F} + \frac{\mathbf{M}_\rho}{\Delta t}\mathbf{V}^n + \mathbf{B}\mathbf{P}_0 + \mathbf{B}\delta\mathbf{P}\right) \tag{19}$$

Inserting this into the second line of Eq. (18) gives:

$$-\mathbf{B}^T \left(\frac{\mathbf{M}_\rho}{\Delta t} + \mathbf{K}\right)^{-1} \left(\mathbf{F} + \frac{\mathbf{M}_\rho}{\Delta t}\mathbf{V}^n + \mathbf{B}\mathbf{P}_0 + \mathbf{B}\delta\mathbf{P}\right) + \mathbf{S}\delta\mathbf{P} = -\mathbf{S}\mathbf{P}_0 \tag{20}$$

This means that the static condensation of the velocity allows one solving the problem in two steps:

$$\text{(I)} \quad \left[-\mathbf{B}^T\left(\frac{\mathbf{M}_\rho}{\Delta t}+\mathbf{K}\right)^{-1}\mathbf{B}+\mathbf{S}\right]\delta\mathbf{P} = \mathbf{B}^T\left(\frac{\mathbf{M}_\rho}{\Delta t}+\mathbf{K}\right)^{-1}\left(\mathbf{F}+\frac{\mathbf{M}_\rho}{\Delta t}\mathbf{V}^n+\mathbf{B}\mathbf{P}_0\right)-\mathbf{S}\mathbf{P}_0 \tag{21}$$

$$\text{(II)} \quad \left(\frac{\mathbf{M}_\rho}{\Delta t}+\mathbf{K}\right)\mathbf{V} = \left(\mathbf{F}+\frac{\mathbf{M}_\rho}{\Delta t}\mathbf{V}^n+\mathbf{B}\mathbf{P}_0+\mathbf{B}\delta P\right) \tag{22}$$

Defining the $\tilde{\mathbf{V}}$ vector as

$$\tilde{\mathbf{V}} = \left(\frac{\mathbf{M}_\rho}{\Delta t}+\mathbf{K}\right)^{-1}\left(\mathbf{F}+\frac{\mathbf{M}_\rho}{\Delta t}\mathbf{V}^n+\mathbf{B}\mathbf{P}_0\right) \tag{23}$$

Static condensation is implemented in the following three steps:

$$\text{(I)} \quad \left(\frac{\mathbf{M}_\rho}{\Delta t}+\mathbf{K}\right)\tilde{\mathbf{V}} = \left(\mathbf{F}+\frac{\mathbf{M}_\rho}{\Delta t}\mathbf{V}^n+\mathbf{B}\mathbf{P}_0\right) \qquad \Rightarrow \tilde{\mathrm{V}} \tag{24}$$

$$\text{(II)} \quad \left[-\mathbf{B}^T\left(\frac{\mathbf{M}_\rho}{\Delta t}+\mathbf{K}\right)^{-1}\mathbf{B}+\mathbf{S}\right]\delta\mathbf{P} = \mathbf{B}^T\tilde{\mathbf{V}}-\mathbf{S}\mathbf{P}_0 \qquad \Rightarrow \delta\mathrm{P} \tag{25}$$

$$\text{(III)} \quad \left(\frac{\mathbf{M}_\rho}{\Delta t}+\mathbf{K}\right)(\mathbf{V}-\tilde{\mathbf{V}}) = \mathbf{B}\delta P \qquad \Rightarrow \mathrm{V} \tag{26}$$

Equations (24–26) represent the way to segregate the pressure from the velocity in a exact way. It is a very expensive procedure from the computational point of view, but if enough resources are available is the correct method to apply. On the other hand, Eqs. (24–26) suggest a procedure to approximate the exact algorithm and to obtain a more efficient way to segregate the pressure.

3.2 Approximation to the Static Condensation

In the Chorin-Teman projection methods, matrix $\mathbf{B}^T\left(\frac{\mathbf{M}_\rho}{\Delta t}+\mathbf{K}\right)^{-1}\mathbf{B}$ in Eq. (25) is approximated by the Laplace matrix L:

$$\mathbf{B}^T\left(\frac{\mathbf{M}_\rho}{\Delta t}+\mathbf{K}\right)^{-1}\mathbf{B} \cong \frac{\Delta t}{\rho}\mathbf{L} \tag{27}$$

where:

$$\mathbf{L} = \int_V \frac{\partial \mathbf{N}}{\partial x_j}\frac{\partial \mathbf{N}^T}{\partial x_j}dV \tag{28}$$

This approximation is acceptable in non viscous or nearly in viscid flows for which matrix $\mathbf{K}$ is negligible versus the mass matrix $\frac{\mathbf{M}_\rho}{\Delta t}$. The remaining matrix

$\mathbf{B}^T \left(\frac{\mathbf{M}_\rho}{\Delta t}\right)^{-1} \mathbf{B}$ is approximately equal to $\frac{\Delta t}{\rho}\mathbf{L}$ (see the definition of $\mathbf{B}$, $\mathbf{M}_\rho$ and $\mathbf{L}$) for a lumped mass matrix and continuous pressure shape functions.

A more suitable way to approximate matrix $\mathbf{B}^T \left(\frac{\mathbf{M}_\rho}{\Delta t} + \mathbf{K}\right)^{-1} \mathbf{B}$ for cases where matrix $\mathbf{K}$ is not negligible will be proposed next.

Being $\mathbf{M} = \sum \mathbf{M}^e$ and $\mathbf{K} = \sum \mathbf{K}^e$ where $\mathbf{M}^e$ and $\mathbf{K}^e$ are the element mass and stiffness matrix corresponding to an element "e". Let us introduce the following approximation in Eq. (25):

$$\mathbf{M}^e \approx \rho^e \mathbf{M}_D^e \tag{29}$$

where $\mathbf{M}_D^e$ is the lumped mass matrix without the ρ

$\mathbf{K}^e \approx \left(\frac{\Delta t \lambda}{J} + \frac{\Delta t G}{J}\right) \frac{1}{h^2} \mathbf{M}_D^e$ in the elastic domain and

$\mathbf{K}^e \approx \frac{\mu}{h^2} \mathbf{M}_D^e$ in the fluid domain.

In case of a moving framework different from the particle displacement, the convective term is added to the fluid lumped stiffness matrix $\mathbf{K}^e$:

$$\mathbf{K}^e \approx \left(\frac{\mu}{h^2} + \frac{|\mathbf{V} - \mathbf{V}_m|}{h}\right) \mathbf{M}_D^e \tag{30}$$

In all previous definitions, h represents a characteristic mesh size, for instance, the average distance between two points.

It must be noted that with the same idea, different possibilities for the lumped mass and stiffness matrices may be proposed. In (29, 30) just the diagonal terms of each matrix are chosen, but other most sophisticated lumped matrices may be used. It is important to repeat that these lumped matrices are used exclusively in the pressure Eq. (25). In Eqs. (24) and (26) the fully consistent matrices are used.

With the previous approximations, the original matrix in Eq. (25) becomes:

$$\left(\frac{\mathbf{M}}{\Delta t} + \mathbf{K}\right)^{-1} = \sum \left(\frac{\mathbf{M}^e}{\Delta t} + \mathbf{K}^e\right)^{-1} \approx \sum \left(\tau^e \left[\mathbf{M}^e\right]_D^{-1}\right) = \mathbf{M}_T^{-1} \tag{31}$$

where $\mathbf{M}_T^{-1}$ is a diagonal matrix obtained from the assembly of the elemental contributions $\tau^e \left[\mathbf{M}^e\right]_D^{-1}$, with

$$\tau^e = \left(\frac{\rho_s}{\Delta t} + \frac{\Delta t \lambda}{J h^2} + \frac{\Delta t G}{J h^2}\right)^{-1} \tag{32}$$

in the elastic domain and

$$\tau^e = \left(\frac{\rho_f}{\Delta t} + \frac{\mu}{h^2} + \frac{|\mathbf{V}^e - \mathbf{V}_m^e|}{h}\right)^{-1} \tag{33}$$

in the incompressible domain.

The first two approximations may be written as:

$$\mathbf{B}^T \left(\frac{\mathbf{M}_\rho}{\Delta t} + \mathbf{K} \right)^{-1} \mathbf{B} \approx \mathbf{B}^T \mathbf{M}_T^{-1} \mathbf{B} \tag{34}$$

Finally, a third approximation, similar to the classical introduced in projection method will be added:

$$\mathbf{B}^T \mathbf{M}_T^{-1} \mathbf{B} \approx \mathbf{L}(\tau) \tag{35}$$

where $\mathbf{L}(\tau) = \Sigma(\tau^e \mathbf{L}^e)$ being $\mathbf{L}^e$ the elemental Laplace matrices.

Then, the three steps algorithm stand:

$$1. \quad \left(\frac{\mathbf{M}_\rho}{\Delta t} + \mathbf{K} \right) \tilde{\mathbf{V}} = \left(\mathbf{F} + \frac{\mathbf{M}_\rho}{\Delta t} \mathbf{V}^n + \mathbf{B}\mathbf{P}_0 \right) \quad \Rightarrow \tilde{\mathrm{V}} \tag{36}$$

$$2. \quad [-\mathbf{L}(\tau) + \mathbf{S}]\, \delta\mathbf{P} = \mathbf{B}^T \tilde{\mathbf{V}} - \mathbf{S}\mathbf{P}_0 \quad \Rightarrow \delta\mathrm{P} \tag{37}$$

$$3. \quad \left(\frac{\mathbf{M}_\rho}{\Delta t} + \mathbf{K} \right) (\mathbf{V} - \tilde{\mathbf{V}}) = \mathbf{B}\delta\mathbf{P} \quad \Rightarrow \mathrm{V} \tag{38}$$

Of course, Eq. (37) is an approximation to Eq. (25) when $\mathbf{B}^T \left(\frac{\mathbf{M}_\rho}{\Delta t} + \mathbf{K} \right)^{-1} \mathbf{B}$ is replaced by $\mathbf{L}(\tau)$. This approximation introduces en error in the evaluation of the unknown $\mathbf{P}$. In order to diminish this error, an iterative procedure may be used to approximate $\mathbf{P}_0$ by $\mathbf{P}$. Effectively, now the introduction of the arbitrary variable $\mathbf{P}_0$ in Eq. (17) becomes justifiable. Introducing this assumption in a iterative process in which once $\mathbf{P}$ evaluated at the k iteration, then, the next iteration is started with $\mathbf{P}_0 = \mathbf{P}^k$. The error introduced by the approximation to $\mathbf{B}^T \left(\frac{\mathbf{M}_\rho}{\Delta t} + \mathbf{K} \right)^{-1} \mathbf{B}$ becomes negligible when $\delta\mathbf{P} \to 0$.

4 Evaluation of the Laplace Matrix $\mathbf{L}(\tau)$ for FSI Problems

When solving an incompressible fluid–elastic solid interaction problem, the incompressible condition (2) is only applied to the fluid domains. This means that the discretized form $\mathbf{B}_i^T \mathbf{V}_i = 0$ is only affects some degrees of freedom (DOF).

Let us call n_P the total DOF corresponding to the pressure, n_V the total DOF corresponding to the velocity, n_s the velocity DOF corresponds to the solid exclusively (without the interfaces), n_f the velocity DOF corresponding exclusively to the fluid (without the interfaces), and n_{sf} the velocity DOF of the interfaces solid–fluid.

Then matrix $\mathbf{B}^T$ is a matrix of n_P files and n_s columns, but all the columns corresponding to the n_s solid DOF are zero. Matrix $\mathbf{B}^T$ has non-zero columns in the DOF corresponding to the fluid domain and the interfaces.

On the other hand, matrix $\mathbf{M}_T^{-1}$ is a diagonal matrix, with terms:

$$\mathbf{M}_T^{-1} = \left[\left(\frac{\rho_f}{\Delta t} + \frac{\mu}{h^2} + \frac{|\mathbf{V}^{n+1} - \mathbf{V}_m|}{h} \right) \mathbf{M}_D \right]^{-1} \tag{39}$$

in the n_f DOF

$$\mathbf{M}_T^{-1} = \left[\left(\frac{\rho_s}{\Delta t} + \frac{G\Delta t}{Jh^2} + \frac{\lambda \Delta t}{Jh^2} \right) \mathbf{M}_D \right]^{-1} \tag{40}$$

in the n_s DOF and

$$\mathbf{M}_T^{-1} = \left[\left(\frac{\rho_f}{\Delta t} + \frac{\mu}{h^2} + \frac{|\mathbf{V}^{n+1} - \mathbf{V}_m|}{h} + \frac{\rho_s}{\Delta t} + \frac{G\Delta t}{Jh^2} + \frac{\lambda \Delta t}{Jh^2} \right) \mathbf{M}_D \right]^{-1} \tag{41}$$

in the n_{sf} DOF.

Performing the double product $\mathbf{B}^T(\mathbf{M}_T^{-1})\mathbf{B}$, all the terms corresponding to the n_s DOF are zero. Matrix $\mathbf{L}(\tau)$ may be written as:

$$\mathbf{L}(\tau) = \mathbf{B}^T(\mathbf{M}_T^{-1})\mathbf{B} = \mathbf{L}_f(\tau_f) + \mathbf{L}_{sf}(\tau_s) \tag{42}$$

$\mathbf{L}_f(\tau_f)$ is the standard Laplace matrix corresponding to the fluid domain including the interfaces.

$$\mathbf{L}_f\left(\tau_f\right) = \sum (\tau_F^e \mathbf{L}^e) \tag{43}$$

$\mathbf{L}_{\mathrm{sf}}(\tau_s)$ is a Laplace matrix corresponding only to the fluid–solid interfaces:

$$\mathbf{L}_{sf}\left(\tau_s\right) = \sum \left(\tau_s \mathbf{L}_{sf}^e\right) \tag{44}$$

where

$$\mathbf{L}_{sf}^e = \int_V \frac{\partial \mathbf{N}_{\mathrm{sf}}}{\partial x_j} \frac{\partial \mathbf{N}_{\mathrm{sf}}^T}{\partial x_j} dV \tag{45}$$

is the Laplace matrix of the solid elements evaluated only with the shape functions $\mathbf{N_{sf}}$ that are different from zero on the fluid–solid interface.

Equation (42) may be also written as:

$$\mathbf{L}(\tau) = \mathbf{L}_f(\tau_f) + \mathbf{L}_{sf}(\beta \tau_f) \tag{46}$$

with

$$\beta = \frac{\tau_s}{\tau_f} = \frac{\frac{\rho_f}{\Delta t} + \frac{\mu}{h^2} + \frac{|\mathbf{V}^{n+1} - \mathbf{V}_m|}{h}}{\frac{\rho_s}{\Delta t} + \frac{G\Delta t}{Jh^2} + \frac{\lambda \Delta t}{Jh^2}} \tag{47}$$

This means that the Laplace interface matrix $\mathbf{L}_{\mathrm{sf}}(\beta \tau_f)$ becomes negligible for small values of the β parameter. This is for instance the case when $\rho_s >> \rho_f$ and the added-mass effect is not present. However, for other physical properties the β parameter may not be negligible, and the Laplace interface matrix must be evaluated in order to obtain good results.

5 The Partitioned (or Staggered) Scheme

Partitioned schemes are based in dividing the original FSI problem in two parts: the solid one and the fluid one. The division is performed independently of using or not sub-iterations in a strongly coupled partitioned scheme or in a loosely coupled one. The idea is exactly the same as for the pressure segregation procedure described above in which the system was split in the velocity and pressure unknowns. Now the same system of equations is split in the solid unknowns (for instance the velocity or the displacements) and the fluid unknowns (normally the velocity and the pressure). Both systems are solved separately.

Let us call $\mathbf{V}_s$ the vector containing the solid unknowns, $\mathbf{V}_f$ and $\mathbf{P}$ the vectors containing the fluid unknowns, not including the common solid–fluid unknowns, and $\mathbf{V}_{sf}$ the vector including the common solid–fluid unknowns.

The transfer of information occurs on the boundary Γ_{SF} by using techniques that guarantee momentum and energy conservation [2]. For staggered algorithms the use of non-matching meshes is a common practice since both systems, fluid and structure, are completely decoupled. The classical boundary conditions at the interface are:

$$(\mathbf{V}_f - \mathbf{V}_s)^T n = 0 \quad on \quad \Gamma_{f-s} \tag{48}$$

$$\boldsymbol{\sigma} n + \mathbf{t}_s = 0 \quad on \quad \Gamma_{f-s} \tag{49}$$

where Eq. (48) represents the consistency condition. Since the interface is modelled using a fully Lagrangian frame of reference this condition guarantees that the fluid and solid meshes will remain tightly coupled along the FSI interface. Equation (49) represents the equilibrium of normal stresses along the interfaces.

The original FSI Eq. (15) may be then written as:

$$\begin{bmatrix} \left(\frac{\mathbf{M}_\rho}{\Delta t} + \mathbf{K}\right)_s & \left(\frac{\mathbf{M}_\rho}{\Delta t} + \mathbf{K}\right)_{sf} & 0 & 0 \\ \left(\frac{\mathbf{M}_\rho}{\Delta t} + \mathbf{K}\right)^T_{sf} & \left(\frac{\mathbf{M}_\rho}{\Delta t} + \mathbf{K}\right)_{ssff} & \left(\frac{\mathbf{M}_\rho}{\Delta t} + \mathbf{K}\right)_{fs} & -\mathbf{B}_{sf} \\ 0 & \left(\frac{\mathbf{M}_\rho}{\Delta t} + \mathbf{K}\right)^T_{fs} & \left(\frac{\mathbf{M}_\rho}{\Delta t} + \mathbf{K}\right)_f & -\mathbf{B}_f \\ 0 & -\mathbf{B}^T_{sf} & -\mathbf{B}^T_f & 0 \end{bmatrix} \begin{bmatrix} \mathbf{V}_s \\ \mathbf{V}_{sf} \\ \mathbf{V}_f \\ \mathbf{P} \end{bmatrix} = \begin{bmatrix} \left(\mathbf{F} + \frac{\mathbf{M}_\rho}{\Delta t}\mathbf{V}^n\right)_s \\ \left(\mathbf{F} + \frac{\mathbf{M}_\rho}{\Delta t}\mathbf{V}^n\right)_{sf} \\ \left(\mathbf{F} + \frac{\mathbf{M}_\rho}{\Delta t}\mathbf{V}^n\right)_f \\ 0 \end{bmatrix} \tag{50}$$

In the monolithic method previously described with pressure segregation, Eq. (50) was partitioned in (a) the three first rows and columns and (b) in the fourth row and fourth column. In classical staggered methods, Eq. (50) is partitioned in the first two rows and columns and then in the other two rows and columns.

For each sub iteration, the static condensation of the terms

$$\mathbf{B}^T_{sf} \left(\frac{\mathbf{M}}{\Delta t} + \mathbf{K}\right)^{-1}_{ssff} \mathbf{B}_{sf} \tag{51}$$

must be taken into account when the added-mass effect is strong.

Using the same conclusion reached in Section 4, an interface Laplace matrix $\mathbf{L}_{\mathrm{sf}}(\beta\tau_f)$ must be added when solving the incompressible part of the domain. Since the meshes on the interface may be non-matching special care has to be taken when Eqs. (39–41) are evaluated. In the general case Eq. (41) takes the form:

$$\mathbf{M}_T^{-1} = \left[\left(\frac{\rho_f}{\Delta t} + \frac{\mu}{h^2} + \frac{|\mathbf{V}^{n+1} - \mathbf{V}_m|}{h} \right) \mathbf{M}_{Df} + \left(\frac{\rho_s}{\Delta t} + \frac{G\Delta t}{Jh^2} + \frac{\lambda \Delta t}{Jh^2} \right) \mathbf{M}_{Ds} \right]^{-1} \quad (52)$$

In conclusion, matrix $\mathbf{L}_{\mathrm{sf}}(\beta\tau_f)$ must be added to the fluid equation, independently of the method used to solve the incompressibility condition. This means that independently of using or not pressure segregation, the fluid solution must include the interface Laplace matrix. This is because, when using a partitioned solution, pressure segregation is implicitly included in the procedure as explained in Eq. (50).

6 Fluid Column Interacting with an Elastic Solid Bottom

The example is a very simple 1D problem for which an analytical results can be easily obtained. Nevertheless from the numerical point of view it has some convergence problems. The example is ideal to test different materials and time step sizes in order to check the validity of the algorithm proposed, in particular the effectiveness of the interface matrix to improve the convergence rate.

The example consistsin an incompressible column over an elastic solid (Fig. 1).

Both column walls have the horizontal displacement constrained (plane strain). The upper line is a free surface and the bottom one has the displacement constrained. Initially, the example had the following physical properties. $\nu = 0.4$; $\mu_f = 0$, $\rho_s = 1500[kg/m^3]$; $\rho_s = 1000[kg/m^3]$, $E_s = 2.3 \times 10^5 [kg/m.\mathrm{sec}^2]$.

The gravity was fixed to $g = -10\,[\mathrm{m/s}^2]$ in the vertical direction and the geometry was discretized as a 2D problem using a mesh of x three-noded linear triangles with $\mathrm{h} = 0.025\,[\mathrm{m}]$.

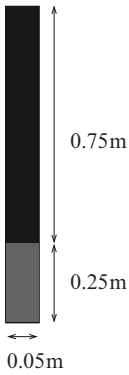

Fig. 1 Water column with an elastic beam

The numerical solution does not converge when the interface Laplace matrix $\mathbf{L}_{\mathrm{sf}}(\beta\tau_f)$ is neglected ($\beta = 0$). The best way to see the importance of this matrix is to study different situations for different densities, different Young modulae and different time steps.

Table 1 shows the performance of the algorithm for a stiff material with a Young modulus similar to steel and different density rates. We can observe that $\beta = 0$ is acceptable only for density rates larger than 6. The number of iterations to achieve the same error is equal to 20 in all cases for $\beta \neq 0$ but it is larger than 40 iterations for $\beta = 0$. This means that even in the case of a FSI problems involving steel and water ($\frac{\rho_s}{\rho_f} = 7$), $\beta \neq 0$ must be used. Probably only in aero-elasticity applications where the density rate is larger than 1,000 the omission of the interface Laplace matrix is justified.

$$E_s = 2 \times 10^{11} \left[\frac{kg}{m\,\mathrm{s}^2} \right]; \quad \nu = 0.3 \quad \Delta t = 10^{-5}[\mathrm{s}]$$

Table 2 shows the same problem for different stiffness properties for the elastic domain but with the density rate fixed to one. This means that the density in the elastic solid and in the fluid is the same. Due to the oscillatory behaviour of the problem, the time step ($\Delta t\,[\mathrm{s}]$) must be changed in order to achieve reasonable time integration with a minimum of time steps for each oscillation. We observe that only for very high Young modulus the case with $\beta = 0$ converges.

Table 1 Iterations to achieve convergence for different density rates

$\frac{\rho_s}{\rho_f}$	$\beta \neq 0$	$\beta = 0$
10	20 iterations	20 iterations
7	20 iterations	More than 40 iterations
6	20 iterations	More than 40 iterations
5	20 iterations	Does not converge
3	19 iterations	Does not converge
1	18 iterations	Does not converge

Table 2 Iterations to achieve convergence for different Young modulus

$E\,(\frac{kg}{m^2})$; $(\Delta t\,[\mathrm{s}])$	$\beta \neq 0$	$\beta = 0$
2×10^{13}; (0.2×10^{-5})	10 iterations	More than 40 iterations
2×10^{12}; (0.5×10^{-5})	14 iterations	Does not converge
2×10^{11}; (1×10^{-5})	18 iterations	Does not converge
2×10^{8}; (1×10^{-4})	40 iterations	Does not converge
2×10^{7}; (1×10^{-3})	36 iterations	Does not converge
2×10^{6}; (1×10^{-3})	40 iterations	Does not converge
2×10^{6}; (1×10^{-2})	34 iterations	33 iterations
2×10^{5}; (1×10^{-2})	36 iterations	Does not converge

Table 3 Iterations to achieve convergence for different time steps

Δt (s)	$\beta \neq 0$	$\beta = 0$
2×10^{-5}	23 iterations	21 iterations
1×10^{-5}	20 iterations	More than 40 iterations
0.75×10^{-5}	18 iterations	Does not converge
0.5×10^{-5}	16 iterations	Does not converge
0.25×10^{-5}	11 iterations	Does not converge

$$\frac{\rho_s}{\rho_f} = 1; \quad \nu = 0.3$$

The most worrisome results are those presented in Table 3. They correspond to a standard steel elastic modulus with a density rate equal to 7. We use first the correct time step size for this kind of problem and see that both formulations for $\beta = 0$ and $\beta \neq 0$ converge reasonably well in 21 iterations. Nevertheless, halving the time step, the number of iterations with $\beta = 0$ duplicates. Decreasing the time step further, the method with $\beta = 0$ does not converge, while the algorithm with the interface Laplace matrix converges in a decreasing number of iterations as expected.

$$\frac{\rho_s}{\rho_f} = 7; \quad E_s = 2 \times 10^{11} [\frac{kg}{ms^2}] \quad \nu = 0.3$$

This example shows that even when classical materials like steel and water are involved, the use of the interface Laplace matrix is recommended to avoid possible difficulties when the time step is smaller than necessary.

The problems were tested with both methods: monolithic with pressure segregation and with a strongly coupled partitioned scheme, with similar conclusions for both cases.

7 Conclusions

The pressure segregation method proposed for the solution of FSI problems with special emphasis in added mass effects has shown an excellent behaviour with promising possibilities in the field of bio-medical applications.

The method was extended to strongly coupled partitioned schemes with the same excellent results. This allows us to conclude that a correct understanding of the pressure segregation is the key issue to solve any FSI problem with either a partitioned or a coupled scheme.

A key feature of the formulation proposed is to learn how to segregate the pressure in the monolithic scheme in order to correctly solve the staggered FSI problem.

Based on the pressure segregation scheme, we have proposed an interface Laplace matrix that gives excellent convergence rates for all the examples studied, even in those cases where the added mass effect is important.

References

1. Felippa CA, Park KC (1980) Staggered transient analysis procedures for coupled-field mechanical systems: formulation. Comput Meth Appl Mech Eng 24:61–111
2. Farhat C, Leisoinne M, LeTallec P (1998) Load and motion transfer algorithms for fluid/structure interaction problems with non-matching discrete interfaces: momentum and energy conservation, optimal discretization and application to aeroelasticity. Comput Meth Appl Mech Eng 157:95–114
3. Piperno S, Farhat C (2001) Partitioned procedures for the transient solution of coupled aeroelastic problems- Part II. Comput Meth Appl Mech Eng 190:3147–3170
4. Neumann M, Tiyyagura SR, Wall WA, Ramm E (2006) Robustness and efficiency aspects for computational fluid structure interaction. Computational Science and High Performance Computing II, Springer, Berlin /Heidelberg, ISSN 1612–2909, vol. 91
5. Lohner R, Yang C, Cebral J, Baum JD, Luo H, Pelessone D (1995) Fluid–structure interaction using a loose coupling algorithm and adaptive unstructured grids. In: Oshima K, Hafez M (eds) Computational Fluid Dynamics Review, Wiley, Chichester
6. Rugonyi S, Bathe KJ (2000) On the analysis of fully-coupled fluid flows with structural interactions–a coupling and condensation procedure. Int J Comput Civil Struct Eng 1:29–41
7. Rugonyi S, Bathe KJ (2001) On finite element analysis of fluid flows fully coupled with structural interactions. Comput Model Simulat Eng (CMES) 2:195–212
8. Souli M, Ouahsine A, Lewin L (2000) Arbitrary Lagrangian–Eulerian formulation for fluid–structure interaction problems. Comput Meth Appl Mech Eng 190:659–675
9. Le Tallec P, Mouro J (2001) Fluid structure interaction with large structural displacements. Comput Meth Appl Mech Eng 190:3039–3067
10. Felippa CA, Park KC, Farhat C (2001) Partitioned analysis of coupled mechanical systems. Comput Meth Appl Mech Eng 190:3247–3270
11. Walhorn E, Kolke A, Hubnerm B, Dinkler D (2005) Fluid–structure coupling within a monolithic model involving free surface flows. Comput Struct 83:2100–2111
12. Dettmer W, Peric D (2006) A computational framework for fluid–structure interaction: finite element formulation and applications. Comput Meth Appl Mech Eng 195:5754–5779
13. Causin P, Gerbeau JF, Vobile F (2001) Added-mass effect in the design of partitioned algorithms for fluid-structure problems. Comput Meth Appl Mech Eng 194(42–44):4506–4527
14. Badia S, Quanini A, Quarteroni A (2008) Splitting methods based on algebraic factorization for fluid-structure interactions. Personal communication
15. Chorin AJ (1968) Numerical solution of the Navier-Stokes equations. Math Comput 22:745–762
16. Temam R (1969) Sur l'approximation de la solution des ̲equations de Navier-Stokes par la methode des pas fractionaires (I). Arch Ration Mech Anal 32:35–153
17. Oñate E (2000) A stabilized finite element method for incompressible viscous flows using a finite increment calculus formulation. Comput Meth Appl Mech Eng 182(1–2):355–370